

# Electronic Band Structure Mapping of Nanotube Transistors by Scanning Photocurrent Microscopy

Eduardo J. H. Lee,<sup>1,\*</sup> Kannan Balasubramanian,<sup>1</sup> Jens Dorfmueller,<sup>1</sup> Ralf Vogelgesang,<sup>1</sup> Nan Fu,<sup>2</sup> Alf Mews,<sup>2</sup> Marko Burghard,<sup>1</sup> and Klaus Kern<sup>1,3</sup>

<sup>1</sup>Max-Planck-Institute for Solid State Research, Heisenbergstrasse 1, 70569 Stuttgart, Germany

<sup>2</sup>University of Siegen, Adolf-Reichwein-Strasse 2, 57068 Siegen, Germany

<sup>3</sup>Institut de Physique des Nanostructures, École Polytechnique Fédérale de Lausanne, CH-1015 Lausanne, Switzerland

(Dated: October 22, 2018)

Spatially resolved photocurrent measurements on carbon nanotube field-effect transistors (CNFETs) operated in various transport regimes are reported. It is demonstrated that the photocurrents measured at different biasing conditions provide access to the electronic band structure profile of the nanotube channel. A comparison of the profiles with the device switched into *n*- or *p*-type states clearly evidences the impact of chemical doping from the ambient. Moreover, we show that scanning photocurrent microscopy constitutes an effective and facile technique for the quantitative determination of the Schottky barrier height in such devices.

PACS numbers: 72.40.+w, 73.63.Fg, 78.67.Ch, 85.35.Kt

Carbon nanotube field-effect transistors (CNFETs) have been extensively studied for applications in electronics and optoelectronics [1, 2]. Despite significant progress in this research field, a range of important device features remain to be fully elucidated, such as the nature of the metal-CNT interface [3]. In this context, scanning probe microscopies can provide relevant local information from devices [4, 5]. A well-suited technique to explore the band structure profile within CNT devices is scanning photocurrent microscopy (SPCM), which so far revealed dominant photocurrent generation at the CNT-metal contacts [6, 7]. Here we report the detailed SPCM characterization of CNFETs in different charge transport regimes, and proof that optical excitation of the nanotubes is the origin of the detected photocurrents. The SPCM data enable convenient access to the height of the Schottky barriers at the contacts. Furthermore, the obtained band profiles are in excellent agreement with current models of CNFET device operation.

SWCNTs were synthesized via chemical vapor deposition (CVD), following the procedure reported by Choi et al [8]. AuPd electrical contacts (15nm thickness) were defined on top the tubes using standard e-beam lithography. Photocurrent and reflection images were simultaneously acquired through a confocal optical microscope coupled to an electrical measurement set-up [6]. Photo-illumination was carried out by a HeNe laser ( $E \sim 1.96$  eV, spot size  $\sim 0.5 \mu\text{m}$ ) with a focused beam intensity of  $\sim 100 \text{ kW/cm}^2$ . The photocurrent measurements were performed under ambient conditions, on a total of 11 different devices.

Figure 1(a) shows the transfer characteristic of a CNFET displaying slightly asymmetric ambipolar behavior. The photocurrent images of the device taken at zero bias in both the *p*- and *n*-type regimes, presented in Fig. 1(b), exhibit enhanced photocurrent responses close to the metal contacts. By contrast, no detectable pho-

toresponse is observed along the entire CNFET device in the OFF state. This difference can be explained by Schottky barriers at the contacts prevalent in the ON states, whereas the flat bands in the OFF-state do not support acceleration of the photo-generated carriers [see insets of Fig. 1(b)]. The gate-induced modulation of the SPCM images solidifies the previous conclusion that built-in electric fields are responsible for the photocurrent generation [6, 7]. Further support for such interpretation stems from the sign of the photocurrent lobes in the various regimes, as exemplified by the line profiles in Fig. 1(c). Based upon the convention that electrons flowing out of the source contact are measured as a positive current, the signs of the photocurrents at the contacts in the ON states of the device are consistent with the direction of the built-in fields there.

Although the photoresponses in the *p*- and *n*-type regimes are qualitatively similar, they exhibit some subtle differences. While in the *p*-type regime, the photocurrent peaks appear almost exactly at the tube/contact interface, in the *n*-type regime they are offset by  $\sim 0.25 \mu\text{m}$  towards the center of the CNT channel. Such a behavior was observed in all of the investigated samples. It demonstrates that the band structure of the device in the *p*-type regime is not just a mirror image of that in the *n*-type regime. To elucidate this further, a series of zero-bias photocurrent images were acquired while sweeping the gate voltage from the *n*-type regime to the *p*-type regime, as depicted in Fig. 2(a). It is apparent that while tuning the device from the *n*-type regime to the OFF state, the photocurrent lobes shift gradually towards the center of the channel, become broader and considerably decrease in intensity. The very low intensity (few tens of pA) features along the channel in the OFF state, observed for some of the samples, may be ascribed to weak local electric fields similar to those observed in metallic CNTs [7]. Such fields could arise due to, e.g.

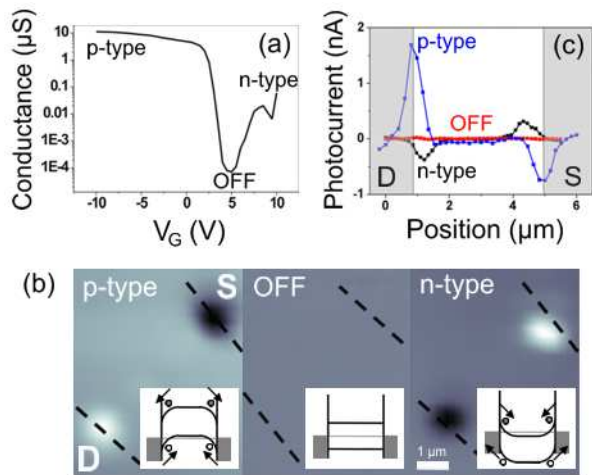


FIG. 1: (a) Conductance *vs.* gate voltage plot of a CNFET (b) Zero-bias SPCM images (white corresponds to positive current). The dashed lines indicate the edges of the source (S) and drain (D) electrical contacts. The insets depict the respective band diagrams. (c) Photocurrent line profiles taken along the nanotube.

defect sites [5]. When the device is further tuned to the *p*-type regime, the lobes appear suddenly at the contacts without showing any gradual movements. This observation is independent of the speed and direction of the gate voltage sweep.

The trend observed upon switching from the *n*-type regime to the OFF state is indicative of lowering and widening of the Schottky barriers. These changes are consistent with theoretical simulations, according to which the Schottky barrier width is closely related to the magnitude of the local electric fields at the contacts [9]. The sudden appearance of the *p*-type lobes in comparison to the gradual movement and broadening of the *n*-type lobes evidences that in the former regime the gate voltage has a much weaker effect on the width of the Schottky barriers. The overall behavior of the CNFET is in close accord with the doped-CNFET model recently proposed by Chen and Fuhrer [10]. It involves chemical *p*-type doping upon nanotube exposure to ambient conditions, thereby introducing a strong band-bending confined to a very small width  $W_{doped}$  for *p*-type operation [Fig. 2(b)] [11]. By comparison, in the *n*-type regime charge depletion occurs over an effective barrier width  $W_{eff}$  of the order of magnitude of the gate oxide thickness  $t$ , which can be effectively modulated by the gate voltage. This situation is different from intrinsic-CNFETs for which in both regimes the bands are bent over a depletion length  $W \sim t$ . Within the doping model, the occurrence of the *p*-type photocurrent lobes at the contacts and the  $\sim 0.25 \mu\text{m}$  shift of the *n*-type lobes [Figs. 1(c) and 2(a)] can be related to the presence of Schottky barriers with respective widths of  $W_{doped}$  and  $W_{eff}$ . Moreover, the

broadening of the lobes upon transition from the *n*-type regime to the OFF-state is attributable to an increase of  $W_{eff}$ , whereas in the *p*-type regime, the absence of such a behavior indicates that the Schottky barrier width is confined to  $W_{doped}$ . Therefore, it is evidenced that the effect of exposure to ambient conditions is not restricted to changes in the metal work function.

Towards the task of determining the band structure profile of CNFETs with the aid of SPCM it has to be ensured that the observed photocurrent signals indeed originate from photoexcitation of the nanotube. Previous CNFET photoconductivity studies have reported photovoltage generation at the Si/SiO<sub>2</sub> interface upon excitation with energies above the Si band gap [2, 12]. To rule out such contributions in the SPCM response, measurements were performed in the *p*-type regime with laser excitation at  $\lambda_{exc} = 1.6 \mu\text{m}$  ( $E \sim 0.78$  eV, spot size  $\sim 2 \mu\text{m}$ ). The obtained SPCM images displayed the same principal features as in the experiments with  $\lambda_{exc} = 633$  nm, proving that the photoresponse predominantly arises from optical excitation of the nanotubes.

In order to determine the Schottky barrier height for holes  $\Phi_{Bp}$ , the gate dependence of the drain current  $I_d$  and the photocurrent at the contacts  $I_{ph}$  was evaluated, following a similar procedure as reported for Si nanowires [13]. The two  $I_{ph}$  curves in Fig. 2(c) cross each other at  $V_G = V_{fb} = 6.9$  V, where  $I_{ph}$  is approximately zero. At this gate voltage, the device is in the OFF state with flat bands at the contacts. Moreover, when  $V_G$  equals the threshold voltage, the drain current reaches zero, corresponding to the situation where the valence band is approximately aligned at the Fermi level [14]. The Schottky barrier height can be calculated as  $\Phi_{Bp} = \alpha_p \cdot (V_{fb} - V_{th})$ , where  $\alpha_p$  is the gate coupling parameter which can be estimated from the subthreshold slope obtainable from the drain current curve in the *p*-type regime [15]. For the sample in Fig. 2, the subthreshold slope is  $\sim 300$  mV/decade, yielding an  $\alpha_p$  value close to 0.2, from which  $\Phi_{Bp}$  is determined to be  $\sim 180$  meV. Similar values have been obtained for other samples. In order to independently determine  $\Phi_{Bp}$ , we have performed temperature dependent  $I - V$  measurements and analyzed the data within the framework of thermionic emission theory, as described in previous works [10, 16]. The measured activation barrier energies at zero bias are shown as a function of  $V_G$  in the inset of Fig. 2(c). In the ON states, the activation energy significantly underestimates the barrier height, since charge injection occurs via thermal-assisted tunneling. On the other hand, in the OFF state, thermionic emission is the dominant process, such that the activation energy approaches  $\Phi_{Bp}$ . Due to sensitivity limitations, a lower limit of  $\sim 170$  meV was estimated for the barrier height, which is in close agreement to the value obtained by SPCM measurements.

Having characterized the devices at zero bias, we now address the effect of finite drain-source bias on the band

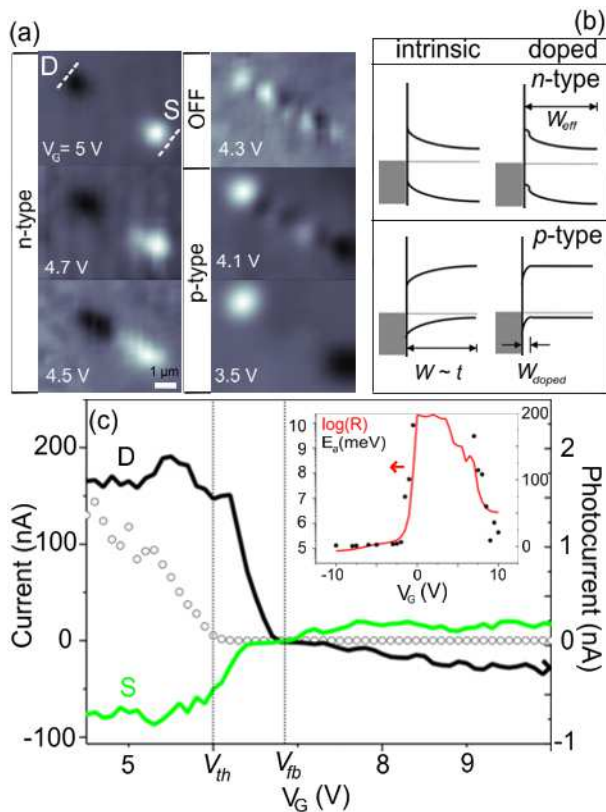


FIG. 2: (a) Zero bias photocurrent response upon transition from the  $n$ - to  $p$ -type. Color scales were normalized such that white (black) corresponds to the maximum (minimum) detected current. (b) Band diagrams depicting the intrinsic and doped-CNFET models. (c) Gate voltage dependence of the drain current (dotted curve) and of the intensity of the photocurrent lobes (solid lines). The inset shows the activation barrier energy at zero bias (dots) and the logarithm of the resistance (red line) as a function of gate voltage.  $V_{th}$  and  $V_{fb}$  correspond to the threshold and flat-band voltages.

structure profile of CNFETs. Figure 3(a) displays a series of SPCM images taken at various bias voltages with the device operated in the  $n$ -type regime. Although a somewhat smaller ratio of photocurrent to the dark current is found in the  $p$ -type regime, the following discussion applies equally well in this case. The images disclose that an applied voltage leads to the enhancement of one of the photocurrent lobes, depending on the sign of the bias. For sufficiently large bias, a single lobe is observed. To better visualize the CNFET band profile, we integrate the photocurrent signal along the length of the tube. This approach is justified by assuming that the photocurrent is directly proportional to the built-in electric field [17]. In Fig. 3(b), the resulting qualitative electrostatic potential profiles are depicted for different bias values, with the source taken as ground and the drain being lifted (lowered) upon application of a negative (positive) potential. It follows from the line profiles that the center

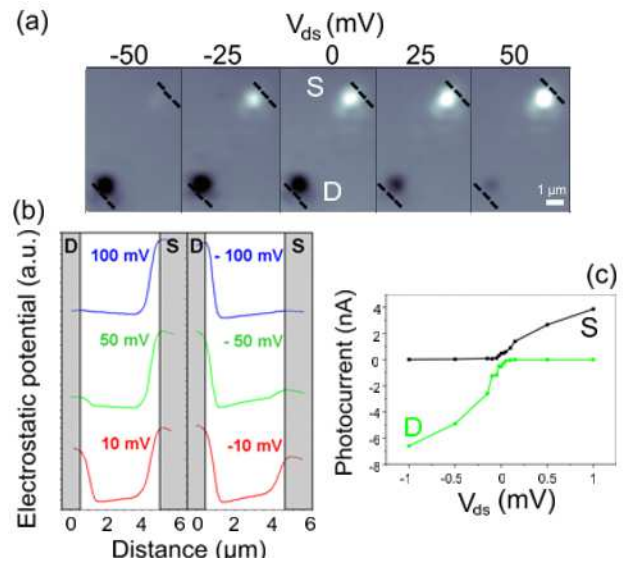


FIG. 3: (a) Effect of bias voltage on the photoresponse in the  $n$ -type ON state. (b) CNFET electrostatic potential profiles taken along the tube. (c) Bias dependence of the photocurrent response at the contacts.

of the channels remains approximately flat irrespective of the applied bias. Moreover, application of a more positive (negative) bias results in a voltage drop predominantly occurring at the source (drain). The band profile changes with increasing bias closely following the behavior expected for the  $n$ -type unipolar operation mode of a CNFET, confirming that the charge transport through the CNT is governed by the contacts. Furthermore, the photocurrent at the lobes  $I_{ph}$  is plotted as a function of  $V_{ds}$  in Fig. 3(c). The  $I_{ph}$ - $V_{ds}$  curves are characteristic of reverse-biased Schottky diodes under photoexcitation [18].

Finally, the effect of gate voltage on the photoresponse of biased CNFETs was investigated. To this end, a series of images similar to those in Fig. 2 were recorded at an applied bias of  $V_{ds} = +0.7$  V, which are collected in Fig. 4(a). At the starting point of  $V_G = 10$  V in the  $n$ -type regime, a single lobe at the source contact is observed, in close correspondence to the situation in Fig. 3(a). Upon decreasing  $V_G$ , the intensity of this lobe gradually decreases and clear photocurrent signals emerge along the tube between the contacts. Around  $V_G = 3.7$  V,  $p$ -type operation sets in and a single lobe emerges at the drain contact, analogous to the observation in Fig. 3(a). The set of SPCM images provides a complete picture of the photoconductivity in CNFETs, in close agreement with a previously proposed model [19]. A major conclusion is that true photoconductivity from an individual CNT is only observable in the OFF state of the device. In the ON states, the local photoresponse is similar to that obtained from a reverse-biased Schottky diode.

It can be recognized from the corresponding electro-

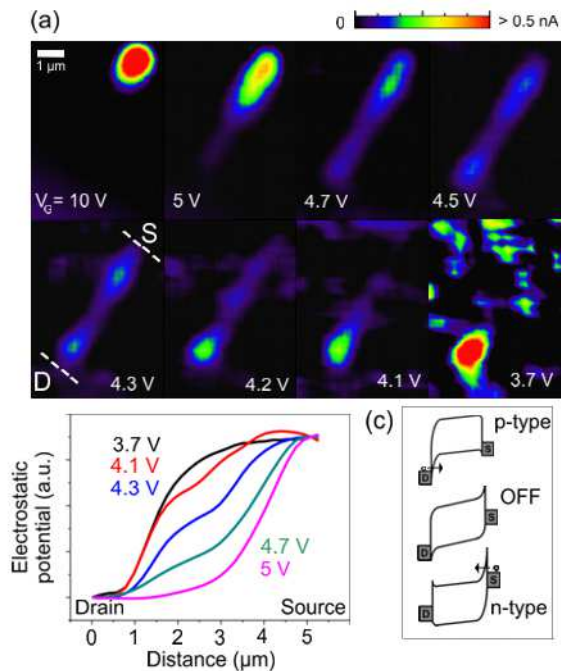


FIG. 4: (a) SPCM images depicting the transition from the  $n$ - to the  $p$ -type regimes taken at  $V_{ds} = 0.7\text{V}$ . (b) Electrostatic potential profiles obtained from the corresponding photocurrent images. (c) Band diagrams describing the different transport regimes of a biased CNFET.

static potential profiles in Fig. 4(b) that in the  $p$ - ( $n$ -) type regime, the voltage drops are concentrated at the drain (source) contact, as opposed to the OFF-state, in which the potential drop is distributed along the entire channel. Closer inspection of the profile at  $V_G = 4.3\text{V}$  suggests that the voltage drop occurring in the vicinity of the contacts is symmetric and stronger than in the middle of the CNT. In total, the band profiles agree very well with the widely accepted model for the operating mechanism of CNFETs, wherein the band structure at the contacts is modulated by the fields induced by gate and drain-source voltages [14]. The band profiles are also consistent with the model used to interpret electroluminescence experiments [20]. Specifically, in the OFF state, the voltage drops at the contacts are symmetric, thus leading to balanced injection of electrons and holes, followed by light emission from the center of the devices. Upon moving away from the OFF state to the  $p$ - ( $n$ -) type regime, the voltage is found to drop mostly at the drain (source) contact, whereby hole (electron) injection is favored. Although the drain bias used in the present experiment is not ideally suited for observing electroluminescence (where  $V_{ds}$  is required to be twice as high as  $V_G$ ), the extracted band profiles describe the underlying scenario impressively well.

In summary, SPCM has been demonstrated to be a versatile tool for CNFET characterization. The obtained photocurrent images confirm the relevance of chemical

doping in CNFETs. Moreover, it has been shown that SPCM allows facile estimation of the Schottky barrier height, for whose determination reliable and straightforward methods are still lacking. The gained values of 150-200 meV are in good agreement with theoretical predictions. Furthermore, SPCM experiments have revealed that photoconductivity can be observed in the OFF state, whereas in the ON regimes the local photoresponse is dominated by the contacts, which behave as photoexcited reverse-biased Schottky diodes.

\* Electronic address: e.lee@fkf.mpg.de

- [1] Ph. Avouris, MRS Bull. **29**, 403 (2004).
- [2] M. Freitag, Y. Martin, J. A. Misewich, R. Martel and Ph. Avouris, Nano Lett. **3**, 1067 (2003).
- [3] Z. H. Chen, J. Appenzeller, J. Knoch, YM Lin, Ph. Avouris, Nano Lett. **5**, 1497 (2005).
- [4] M. Freitag, M. Radosavljevic, Y. X. Zhou, A. T. Johnson, W. F. Smith, Appl. Phys. Lett. **79**, 3326 (2001).
- [5] M. Bockrath, W. Liang, D. Bozovic, J. H. Hafner, C. M. Lieber, M. Tinkham and H. Park, Science **291**, 283 (2001).
- [6] K. Balasubramanian, Y. Fan, M. Burghard, K. Kern, M. Friedrich, U. Wannek and A. Mews, Appl. Phys. Lett. **84**, 2400 (2004).
- [7] K. Balasubramanian, M. Burghard, K. Kern, M. Scolari, A. Mews, Nano Lett. **5**, 507 (2005).
- [8] H. C. Choi, W. Kim, D. Wang and H. Dai, J. Phys. Chem. B **106**, 12361 (2002).
- [9] S. Heinze, J. Tersoff, R. Martel, V. Derycke, J. Appenzeller and Ph. Avouris, Phys. Rev. Lett. **89**, 106801 (2002).
- [10] Y. F. Chen and M. S. Fuhrer, Nano Lett. **6** 2158 (2006).
- [11] F. Leonard and J. Tersoff, Phys. Rev. Lett. **89**, 179902 (2002).
- [12] M. S. Marcus, J. M. Simmons, O. M. Castellini, R. J. Hamers and M. A. Eriksson, J. Appl. Phys. **100**, 084306 (2006).
- [13] Y. Ahn, J. Dunning and J. Park, Nano Lett. **5**, 1367 (2005).
- [14] J. Appenzeller, J. Knoch, V. Derycke, R. Martel, S. Wind and Ph. Avouris, Phys. Rev. Lett. **89**, 126801 (2002).
- [15] S. Rosenblatt, Y. Yaish, J. Park, J. Gore, V. Sazanova and P. L. McEuen, Nano Lett. **2**, 89 (2002).
- [16] R. Martel, V. Derycke, C. Lavoie, J. Appenzeller, K. K. Chan, J. Tersoff and Ph. Avouris, Phys. Rev. Lett. **87**, 256805 (2001).
- [17] The electrostatic potential profile is valid only in the region between the contacts. Moreover, it is broadened by convolution with the Airy pattern of the incident laser beam.
- [18] Y. Gu, E. S. Kwak, J. L. Lensch, J. E. Allen, T. W. Odom and L. J. Lauhon, Appl. Phys. Lett. **87**, 043111 (2005).
- [19] K. Balasubramanian and M. Burghard, Semicond. Sci. Technol. **21**, S22 (2006).
- [20] M. Freitag, J. Chen, J. Tersoff, J. C. Tsang, Q. Fu, J. Liu and Ph. Avouris, Phys. Rev. Lett. **93**, 076803 (2004).